*Chapter 2*

# Solar thermal energy systems

## *2.1. Introduction*

Technologies for wider use of renewable energies must be simple and reliable, affordable in developing countries with low technological development, which have exportable and technical solar potential, but resources of materials are limited. They must produce more energy during their life, should not deplete natural resources, and should not create products that have a negative impact on the society or the environment.
Solar energy can be converted in two ways:

- By thermal conversion (solar energy is converted into heat energy, used for heating, domestic water or electricity production);
- By using the photovoltaic effect (directly convert solar energy into electricity).

There is a wide variety of technical means to convert solar radiation into thermal energy, which can be divided into two groups:

1. Systems for direct and diffuse solar energy conversion into thermal energy at low temperatures. These do not require tracking the sun and have a simple construction. This group includes:

- Flat-plate solar collector for water and air heating;
- Flat-plate solar collector– flow turbine system (solar towers);

The last system are used to generate electricity.

2. Systems with solar radiation concentration, which convert the direct component of solar radiation into thermal energy under average and high temperatures (from several hundred to several thousand degrees). This group includes:

- Linear-parabolic (trough) systems;
- Paraboloidal systems with different types of engines (steam turbine, Sterling engine, etc.);
- Central receiver  collector systems or “Power Tower”.

In most cases concentration systems are used to produce electricity (Concentrated Solar Power - CSP). Linear-parabolic systems track the sun as a single coordinate. A distinctive feature of CSP consists in multiple energy conversion: solar radiation is converted into heat, then, using Carnot thermodynamic cycle or others, the heat is converted into mechanical energy. Finally, the electromechanical conversion is used to obtain electricity. From this point of view, photovoltaic conversion is superior compared to CSP – solar radiation is converted directly into electricity.

In all systems, solar radiation can be absorbed by a flat collector or can be concentrated optically using mirrors and lenses. Optimal choice depends on the technological-energy needs, location and weather conditions.

Weather effects and solar altitude angle have a major impact on the efficiency of concentrating collectors, which use only direct rays of the sun. In Fig. 2.1 the power production as function of month is presented [1].

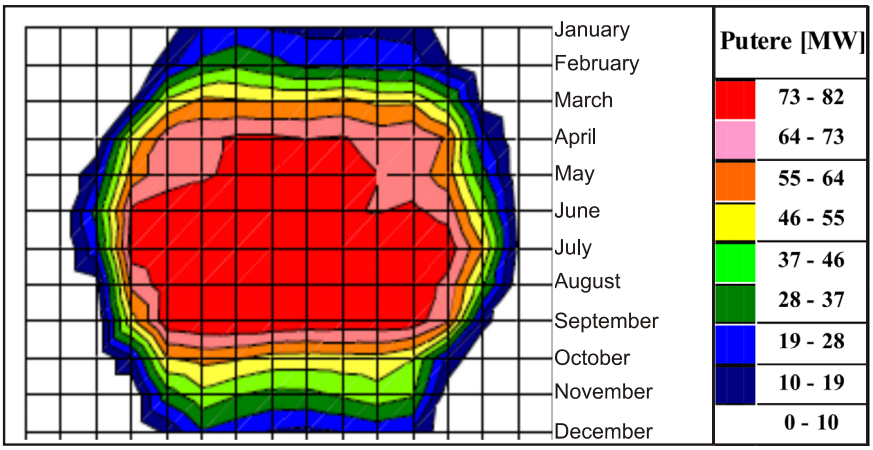


**Fig. 2.1.** Typical average production of power by SES

## *2.2. Solar systems for water heating*

### 2.2.1. Brief history

**Thermal conversion** is the oldest and most widespread form of solar energy utilization. The first attempts to use solar energy for heating were made in Greece in the fifth century before Christ. At that time, the Greeks had already succeeded to exhaust their forestry resources and firewood was imported from Macedonia, Cyprus and the Middle East. With the discovery of glass by the Romans, the development of bioclimatic concepts in buildings' construction started, which purpose was the efficient use of natural lighting, aeration (ventilation) of spaces in hot regions or heating the spaces in areas with moderate climates, using solar energy. The discovery of the greenhouse effect at the end of the eighteenth century, followed by the experiments undertaken by Horace de Saussure's (Switzerland, 1767), Augustine and Abel Mouchot Pifre (France, 1870), contributed to the first successful commercial systems for hot water production by using solar power (California, early twentieth century), then in Florida (between 1920-1950), water pumping, Frank Shuman (Egypt, 1912) [2-4].

Any black surface exposed to solar radiation, called absorbing surface, transforms solar energy into heat. This absorbing surface is the simplest example of direct converter of solar radiation into thermal energy, called **"flat solar collector".** Solar thermal energy conversion includes several technologies: water heating with flat or vacuum collectors, drying agricultural products and medicinal plants, and in semi-finished wood processing, solar refrigeration, distillation of water, electricity generation, using thermodynamic process, etc.

**Technological aspects.** Over the centuries, engineers and architects have improved the design of buildings for the most rational use of natural light and heat source - the Sun. From this point of view, the walls of buildings are heat accumulators, and the windows and rooms - are heat collectors, which allow penetration of visible band (short wave) solar radiation in the inside and do not allow infrared radiation (long wave) to leave the building. This technology, and, respectively, the systems used to achieve it were later called passive systems or methods to use solar energy. Passive systems are distinguished by the following two distinct features:

1. The processes for collecting, storing and using energy are integrated into the building structure. In other words, Sun radiation heat the consumer directly;
2. Passive systems do not require mechanical energy to transport heat to the consumer or storage tank. Motion of air flows takes place under temperature differences between different layers.

On the contrary, active systems for solar energy conversion are equipped with special solar collectors in which solar radiation is converted into heat, and then through a heat carrier (usually water or air) is transported to the consumer or stored in the tank. The most common types of solar collectors are flat solar collectors used to obtain maximum temperatures up to 150ºC.

### 2.2.2. Flat solar collector for water or air heating at small temperatures

Solar collector is a special heat exchanger that transforms the energy of solar radiation into thermal energy. Also, the solar collector differs from most conventional heat exchangers (e.g., liquid-liquid heat exchangers), in which the heat transfer by radiation plays an insignificant role. In the solar collector, on the contrary, energy transfer to the liquid or gas is carried away through solar radiation with the wavelength ranging between 0,3 and 3 μm, and maximal power density of 1000-1100 W/m2.

Flat-shaped solar collector can be designed to supply hot water at low temperatures of about 40-150 ºC. It uses both components of solar radiation - direct and diffuse, it does not require tracking the sun in the sky, it generates low operating costs and has a much simpler construction compared to collectors with solar radiation concentration. This type of collector is the most widespread, as it is part of any water heating system, of residential areas, of solar drying chambers and refrigeration systems. It is technically and technologically highly advanced, and has a developed market and economic prospects. Fig. 2.2 shows the design scheme of a solar collector for water heating. Its main components are: the so-called "black box" 5 with thermal insulation 4 of three walls, coated on the front by transparent surface (TS) 3.

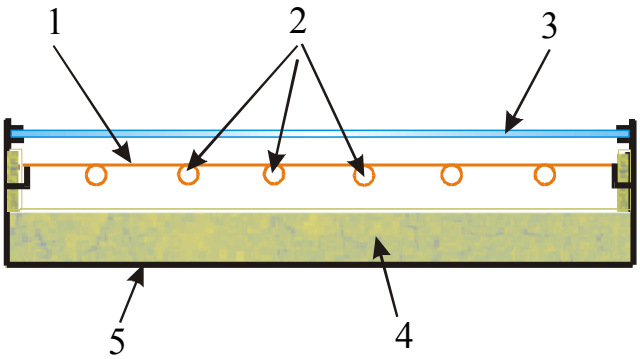


**Fig. 2.2.** Constructive schema of the solar collector

Heat exchanger is metal plate-pipe type, absorbent surface (AS) 1 and pipes 2, respectively. In the case of the air collector, the heat exchanger is metal plate-air channel. The solar collector operates based on two physical phenomena: absorption of solar radiation by a black body (Fig. 2.2, absorbing surface 1) and the greenhouse effect performed by the transparent surface 3. Artificial greenhouse effect is made in the case of the solar collector. Surface 3 is transparent to sun radiation and opaque to infrared radiation that is heat, emitted by the AS 1. AS temperature increases and heat is transmitted to water running through pipes 2. Plate-pipe type heat exchanger is the main element of the collector shown in Fig. 2.2.

Over the years, various technical solutions have been proposed for plate 1 – pipes 2 combination. The most viable solutions are shown in Fig. 2.3: serpentine (a), parallel tubes (b), channels consisting of two metal plates by contact method welding (c) or channels formed inside a plastic materiel (d).

In order to reduce heat loss through the space between the AS and TS, the heat exchanger of plate-pipe type is mounted in a glass evacuated-tube. Thus, a significantly lower heat transfer by convection between the AS and TS areas occurs and the collector efficiency increases.

The first evacuated-tube collector has been proposed by Speyer in 1965. Fig. 2.4 shows two design schemes of vacuum collectors. Tightly connected AS 2 and pipe 3 are placed into the glass tube 1.

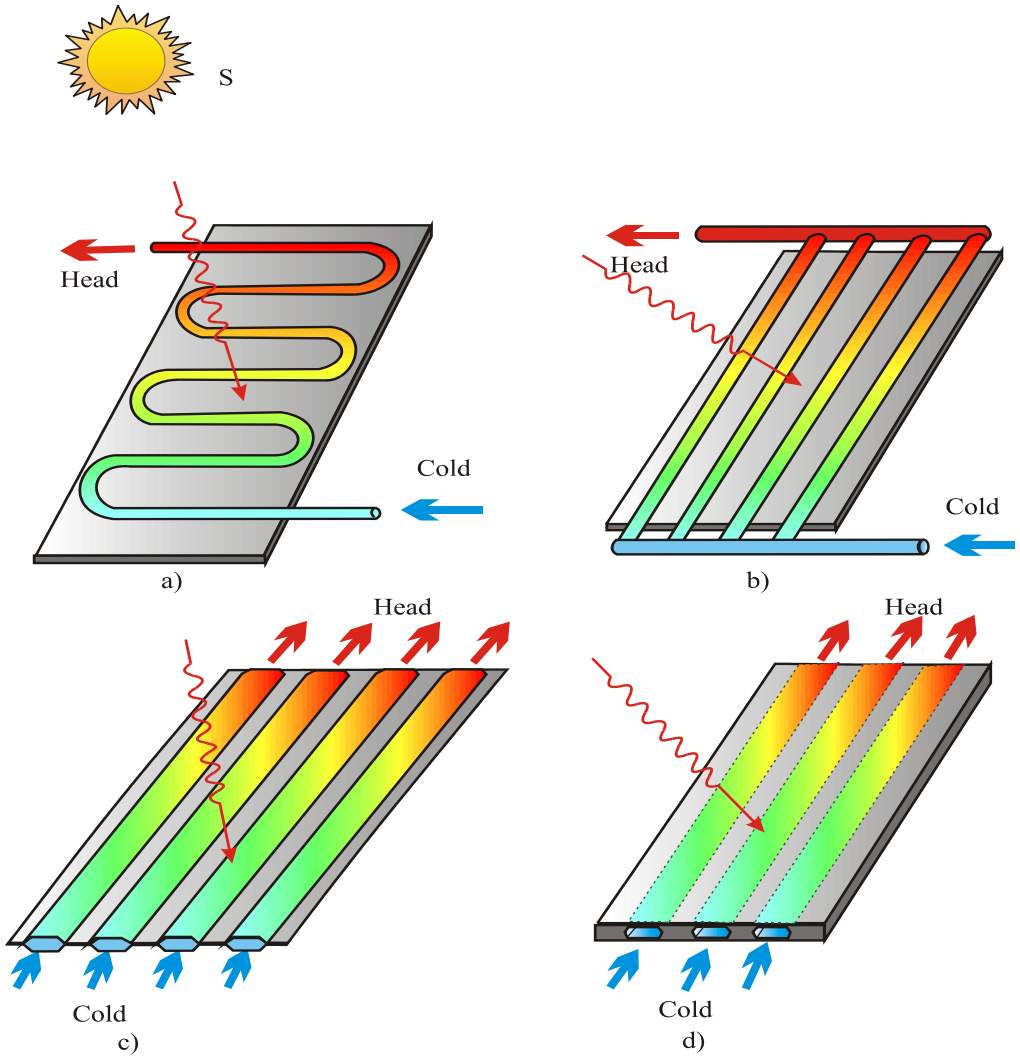


**Fig. 2.3.** Heat exchangers for solar collectors

There is an essential difference between these two schemes. In the a) scheme cold water enters through nozzle 5, is being heated and through nozzle 4 it is transported to the storage tank.

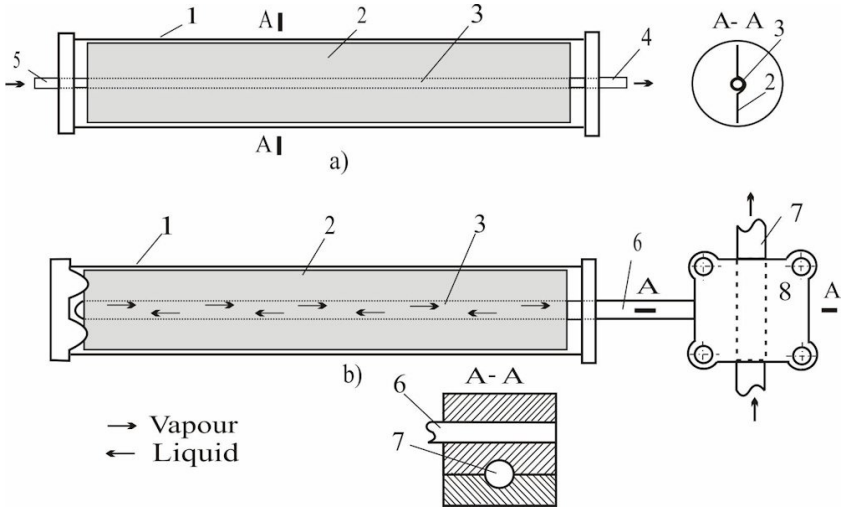


**Fig. 2.4.** Schematic design of evacuated-tube collectors

Both nozzles must be tightly connected to the glass tube. Tube 1 and pipe 3 expand differently, thus causing the loss of tightness between nozzle-glass tube connection. In the

second scheme there is only one tight connection - the end 6 of tube 3. Heat transfer is done in the heat exchanger 8, to which end pipe 6, serving as condenser, and the pipe 7, through which water circulates, are mounted. Pipe 3 is partially filled with a liquid with a relatively low evaporation temperature. Under the action of heat absorbed by plate 2, the liquid evaporates, pressure increases and vapour move to the capacitor condenser - the end of pipe 6. Here vapour condense giving heat to water flowing through the pipe 7. The liquid from the condenser flows in the opposite direction through pipe 3. Evacuated-tube solar collector contains several tubes connected in parallel and mounted into a common frame to form a register. Disadvantages of evacuated-tube collectors: they are about 1,5 times more expensive, have a greater mass; there is a risk of deterioration of tight connections that cannot be repaired under service conditions.

Schematic diagram of air heating solar collector is similar to the water collector (see Fig. 2.5).

Its main components are: absorbing surface 1, transparent area 2, the thermal insulation 3 and frame 4. Heat transfer takes place between AS and the airflow moving through the channel between TS and AS or between AS and thermal insulation layer, or both. Air density is about 900 times smaller than that of water and a more intensive circulation of air is required. For this, the fan 5 is used to transport cold air to AS and further to the consumer. Thermal conductivity of air is about 25 times smaller than that of water and it is necessary to substantially increase the contact area between TS and the airflow to achieve the same heat transfer. Air heating solar collector differs from that discussed above only by the design of absorbing surface 1. In Fig. 2.6 there are four design options of TS, whose major goal is to increase contact area between air and TS, creation of turbulent air movement and, consequently, increase of heat transfer efficiency:

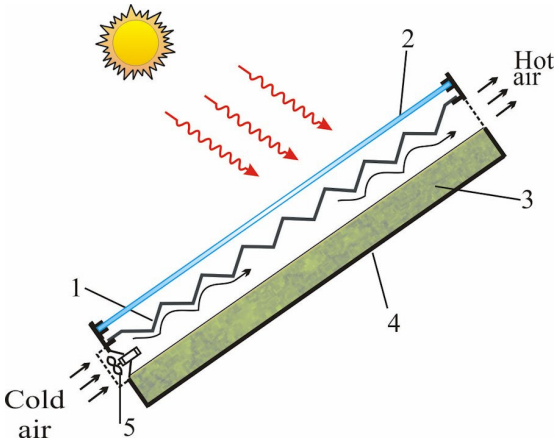


**Fig. 2.5.** Collector schematic disign for air heating

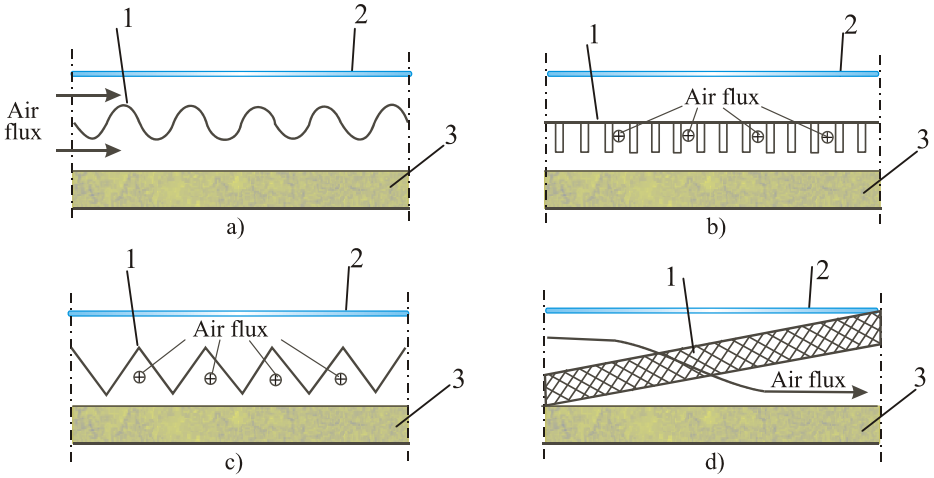


**Fig. 2.6.** Solar collectors for air heating: design of absorbing surfaces

a) wavy surface, air flow moves through both channels;

b) the airflow moves through channels formed from metal plates welded to the rear of AS, forming a register (Fig. 2.6, b, airflow direction is perpendicular to the surface of the page);

c) differs from the previous version of the triangular shape of the channels;

d) AS is composed of metal wire mesh or filled with granular material, through which air flow circulate.

### 2.2.3. Thermal and design characteristics of the solar flat-plate collector

**Standard flat-plate collector efficiency.** Fig. 2.7 presents a simplified energy balance of a standard flat-plate collector. Dimensions of the constructive elements are conventional. From short-wave direct and diffuse global solar radiation *G*, incident on the transparent area *TS*, an important part $\tau G$ determined by the transparency coefficient $\tau$, reaches the absorbing surface *AS,* where it is converted into heat. Transparent surface *TS* reflects radiation $\rho G$ into space and absorbs $\alpha TG$, these values being quantitatively determined by reflectance ratio $\rho$ and, respectively, by the material absorption coefficient $\alpha T$ of material *TS*. Part of the radiation $\tau G$ incident on the absorbing surface *AS* is reflected and the biggest part is converted into heat.

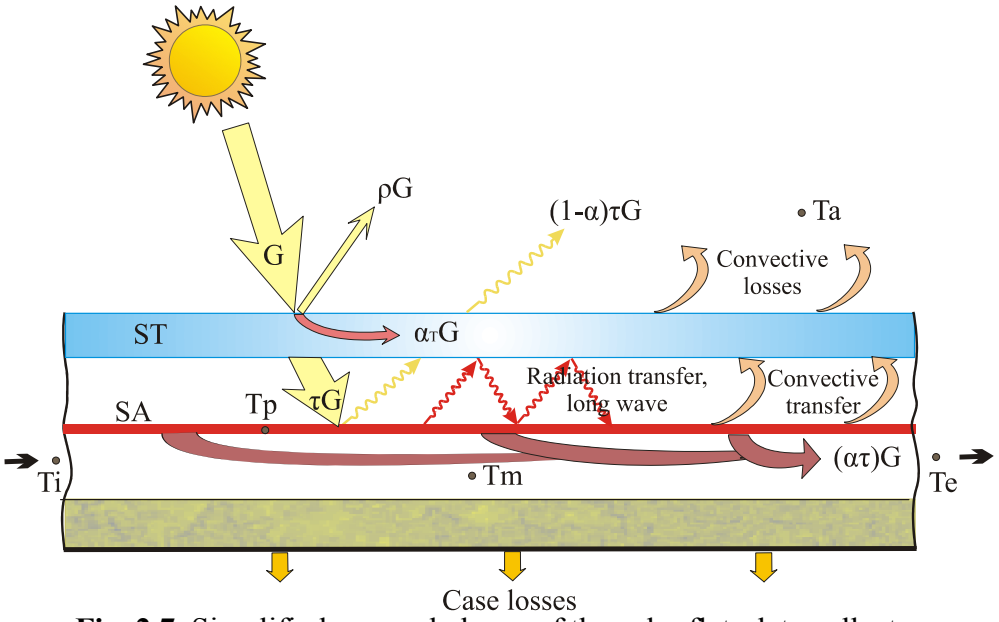


**Fig. 2.7.** Simplified energy balance of the solar flat-plate collector

It is obvious that for TS the sum of $\tau$, $\rho$ and $\alpha_T$ coefficients is:

$$\tau + \rho + \alpha_T = 1. \qquad (3.1)$$

Absorbing surface *AS* absorbs solar radiation, temperature $T_p$ increases to 40-100ºC and *AS* will also radiate energy, but already in the long-wave infrared band, for which *TS* is opaque. Arriving to *TS*, this radiation is partially absorbed, heating the *TS,* and is partially reflected to the surface *AS*. Thus greenhouse effect is simulated by means of *TS* which prevents the emission into space of infrared radiation emitted by *AS*.

Efficiency of converting solar radiation into heat is determined by the absorption coefficient $\alpha$ of the surface *AS*. Only a fraction of global solar radiation *G* will turn into heat, due to material properties of transparent surface *TS* and of the absorbing surface *AS:*

$$P_{SA} = (\alpha\tau)G \qquad (3.2)$$

Power $P_{SA}$ must cover energy losses from the surface *TS*, which take place by convective transfer, as well as by casing losses. These losses are in the first approximation proportional to the temperature difference between $T_p$ of *AS* and that of the environment $T_a$:

$$\Delta P = U_P(T_p - T_a), \qquad (3.3)$$

where $U_P$ is the total loss coefficient, W/m$^2$·$^0$C, ranging from 1 to 30 W/m$^2$·$^0$C.

Useful power generated by solar collectors is determined by the expression, known as Hottel-Whillier-Bliss (H-W-B) [5]

$$P_U = (\alpha\tau)G - U_P(T_P - T_a) \tag{3.4}$$

and thermal efficiency

$$\eta = \frac{P_U}{G} = (\alpha\tau) - U_P \frac{T_P - T_a}{G}. \tag{3.5}$$

From the expression (3.5) follows:

- When $U_P$=const. and $(\alpha\tau)$=const, the efficiency decreases linearly depending on $(T_P-T_a)/G$;
- maximal efficiency is when $T_P=T_a$ and it depends only on the optical properties of the *TS* and *AS* material;
- Global radiation *G* decrease leads to efficiency decrease.

Factor $(\alpha\tau)$ characterizing optical properties of *TS-AS* unit (transparent surface - absorbing surface), provides a classification of solar collectors in terms of efficiency and of overall loss

**Table 2.1.** Characteristics of main flat-plate collector types.

| **Collector type** | **(ατ)** | **Overall loss factor, W/m$^2$· $^0$C** | |
|---|---|---|---|
| | | **Usual interval** | **Average** |
| Selective surface, void tubes, SS–V | 0,7 | 2 - 3 | 2,5 |
| Selective surface, glass sheet, SS–1 | 0,85 | 3 - 5 | 4,0 |
| Black surface, two glass sheets, SN–2 | 0,75 | 4 - 6 | 5,0 |
| Black surface, one glass sheet, SN–1 | 0,85 | 6 - 8 | 7,0 |
| Without transparent surface, FST | 0,95 | 15 - 30 | 20,0 |

coefficient $U_P$. Table 2.1 lists the main types of solar collectors, usual values of $(\alpha\tau)$ factor, and, overall loss coefficient, respectively. Fig. 2.8 presents the evolution of efficiency in terms of temperature difference $T_a$ - $T_P$. The calculation was performed using the expression (3.5) for mean overall loss coefficient and the value of global solar radiation $G$ = 800 W/m$^2$, and the temperature $T_a$ = 20°C.

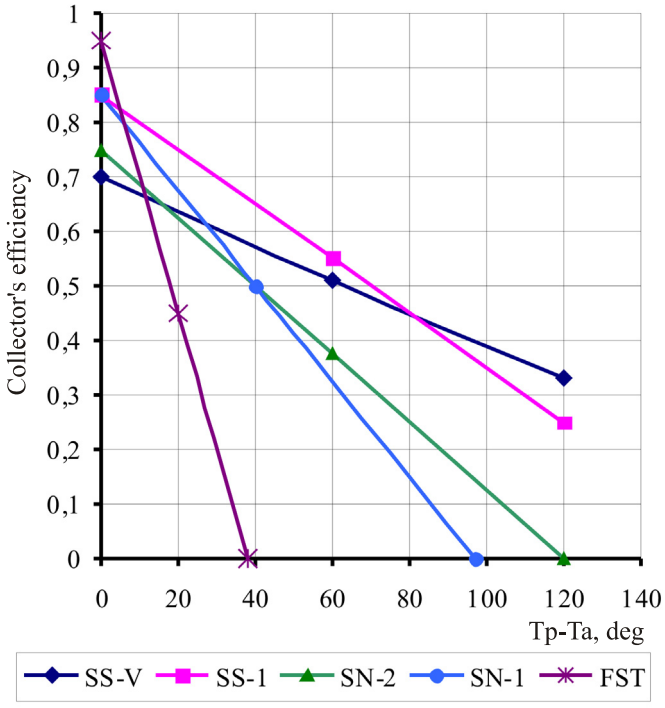


**Fig. 2.8.** Efficiency evolution of various types of solar collectors.

**Common collectors' haracteristics.** Evolution of efficiency from Fig. 2.8 and the characteristics listed in Table 2.1 provide information for comparative analysis of different flat-plate solar collectors' design:

1. The characteristics of SN-1 collector with a black absorbing surface and a glass layer occupy an intermediate position. It is the most frequently used and in the above conditions it allows water heating up to 60 ºC temperature with efficiency between 45 and 50 %. This type of collector is considered, usually, a reference one.

2. By excluding the transparent surface *TS*, the *FST* collector is obtained, called **energy roof**, which increases the factor ($\alpha\tau$), but simultaneously increases the overall loss coefficient $U_P$ due to direct wind exposure and convective heat transfer enhancing. Provides air heating to 40-50 ºC with efficiency between 30 % and 50 %. It is commonly used for drying agricultural products (hay, grain, fruit, vegetables, etc.).
3. By installing two glass layers the collector SN-2 is obtained, which reduces the convective and radiation losses, but decreases the factor ($\alpha\tau$) due to transparency diminution. In the usual $T_P$-$T_a$ temperature differences zone, between 30 and 60 ºC, a significant increase of efficiency does not take place, and the collector is harder and more expensive.
4. Radiation losses can be significantly reduced in SS-1 collector with selective absorbing surface (see next paragraph) and a single glass layer. Here convective losses are dominant.
5. A radical solution to minimize convective losses is to use vacuum tubes. It takes place in the selective surface SS-V collector. This type of collector allows water heating to temperatures above 100ºC.

## 2.2.4. Optical properties of the materials for transparent and absorbing surfaces

As outlined above, maximum efficiency of solar collector or factor ($\alpha\tau$) depends only on the properties of materials used for the absorbing surface or plate *AS*, respectively, for the transparent area *TS*. The solar radiation entering any surface can be absorbed, transmitted through material or reflected (Fig. 2.9).

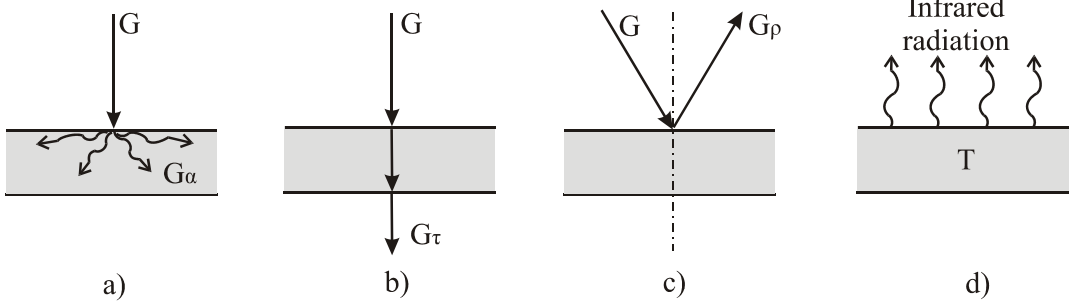


**Fig. 2.9.** Absorption (a), transmission (b) and reflection of short wave radiation (c). A body (surface) with temperature *T* is emitting long wave radiation into the space (d).

The notion of spectral absorption coefficient $\alpha_\lambda$ equal to the ratio of the wavelength $\lambda$ radiation absorbed and radiation incident on the same wavelength is introduced. Coefficient $\alpha_\lambda$ represents a property of matter and does not depend on the radiation property, for example, on the incident radiation wavelength. It just shows what part will be absorbed by the interaction of respective electromagnetic radiation with the material (for solar installations - absorbing surface). Also, the notion of spectral transmittance coefficient $\tau_\lambda$, and that of spectral reflection coefficient $\rho_\lambda$ are introduced.

$$\alpha_\lambda + \tau_\lambda + \rho_\lambda = 1. \tag{3.6}$$

The values of these coefficients are approximately constant in the range of the incidence angle $\theta$ variation between 0 and 60° and decreases sharply for angles greater than 70°.

Given that solar radiation has a broad spectrum of electromagnetic waves, the terms below are used for practical purposes, which reflect the interaction of the material and electromagnetic radiation throughout its range:

1. **Absorbance *α*,** defined as the ratio between the power of the absorbed- and incident solar radiation:

$$\alpha = \frac{G_\alpha}{G}; \tag{3.7}$$

2. **Transmittance *τ*,** defined as the ratio of radiated power transmitted through the respective material and the incident radiated power:

$$\tau = \frac{G_\tau}{G}; \tag{3.8}$$

3. **Reflectance *ρ*,** determined as the ratio of reflected radiated power to incident radiated power:

$$\rho = \frac{G_\rho}{G}. \tag{3.9}$$

Equation (3.7) can be written as follows:

$$\alpha = \frac{\int_0^\infty \alpha_\lambda G_{\lambda\alpha} d\lambda}{\int_0^\infty G_\lambda d\lambda}. \tag{3.10}$$

Similarly coefficients $\tau$ and $\rho$ can be expressed. The relation (3.6) is also respected

$$\alpha + \tau + \rho = 1. \tag{3.11}$$

The coefficients $\alpha$, $\tau$ and $\rho$ characterize the behavior of transparent or absorbing surface at solar radiation action, which represents a spectrum of short waves between 0,3 and 3 μm. They are also called **"optical" or "solar"** coefficients. At the same time, the respective area is heated and generates into space infrared radiation in the range between 3 and 20 μm. This process is characterized by spectral emission coefficient $\varepsilon_\lambda$, called **"radiative"** and defined as the ratio of delivered power flux $W_{\varepsilon\lambda}$ with the wavelength $\lambda$ and the flow of power delivered by an absolutely black body $W_{\lambda n}$ at the same wavelength $\lambda$ and temperature $T$.
According to Kirchhoff's law for any wavelength $\lambda$ and temperature $T$ the following relationship occurs:

$$\alpha_\lambda = \varepsilon_\lambda , \tag{3.12}$$

in other words, a body with temperature $T$ absorbs and emits the same amount of electromagnetic radiation with wavelength $\lambda$.

As defined above, the emission factor or **emittance** for the entire spectrum of radiation is determined similarly to the absorption $\alpha$ (see 3.10):

$$\varepsilon = \frac{\int_0^\infty \varepsilon_\lambda W_{\varepsilon\lambda} d\lambda}{\int_0^\infty W_{\lambda n} d\lambda} = \frac{W_\varepsilon}{W_n} , \tag{3.13}$$

where $W_\varepsilon$, $W_n$ is the flow of power delivered by the real body with temperature $T$, and, respectively, the flow of power delivered by an absolutely black body at the same temperature.

In accordance with expression (2.6), an absolutely black body of $A$ area will emit an power flux $W_n = \sigma \cdot A \cdot T^4$ and, therefore, the flow of radiative losses will be:

$$W_\varepsilon = \varepsilon \cdot \sigma \cdot A \cdot T^4 . \tag{3.14}$$

**Absorbing surface materials.** The ideal material has the following optical properties $\alpha=1,\ \tau=\rho=0$. It is obvious that such a material does not exist. Absorbing surface, being opaque, has transmittance $\tau$ equal to zero. The major part of solar radiation is absorbed and converted into heat and only a small fraction of solar radiation is reflected. Table 2.2 shows absorption and emission characteristics collected from [5-7] for various materials and surfaces. The absorbance of material or the absorbing surface of solar radiation in the short wave range (0,3 to 3,0 μm) was noted with $\alpha_{\text{short}}$ , and $\varepsilon_{long}$ is emittance of the material or surface in the infrared wave range (bigger than 3,0 μm). We conclude that pure metals are not suitable for making absorbing surfaces. Also, aluminum is not recommendable because it may induce very fast electrical corrosion phenomena into the installation circuit. Steel plate covered with black paint has a satisfactory absorption, is cheap, but is not resistant to corrosion.

A special class is formed by the selective materials and surfaces possessing a high absorption coefficient for short waves, and, respectively, a lower emission coefficient for long waves. For these materials, the report $\alpha_{short}t/\varepsilon_{long}>>1$.

**Table 2.2.** Absorbance and emittance of some materials and absorbing surfaces.

| Type of material or absorbing surface | Absorbance, $\alpha_{short}$, short wave | Emittance, $\varepsilon_{long}$, infrared waves | Ratio $\alpha_{short}/\ \varepsilon_{long}$ |
|---|---|---|---|
| **Traditional materials** | | | |
| Pure iron | 0,44 | 0,11 | 4,0 |
| Pure aluminum | 0,10 | 0,10 | 1,0 |
| Polished copper | 0,35 | 0,08 | 8,8 |
| Oxidized steel sheet | 0,74 | 0,82 | 0,90 |
| Steel sheet plated with black paint | 0,95 | 0,95 | 1,0 |
| Graphite (black lead) | 0,78 | 0,41 | 1,90 |
| Carbon black | 0,96 | 0,89 | 1,08 |
| White paint | 0,12-0,18 | 0,93 | 0,13-0,19 |
| **Selective materials and surfaces** | | | |
| Black chromium on a nickel surface | 0,95 | 0,09 | 10,7 |
| Porous ceramic son a steel surface | 0,96 | 0,16 | 6,0 |
| Black nickel oxide (green oxide) on an aluminum surface | 0,85-0,93 | 0,06-0,10 | 14,5-15,5 |
| Copper oxide, $Cu_2O$, on a copper surface | 0,90 | 0,16 | 6,0 |

Fig. 2.10, a, shows the spectral characteristics for various absorbing surfaces; and Fig. 2.10, b, shows the explanation of the selective surface effect. In the spectral range between 0,3 and 3 μm absorbance and emittance of ideal selective surface is equal to 1, and in higher frequencies range over 3 μm - are zero. Copper oxide (selective material) characteristic differs from the ideal one, but there was noticed a small value of emittance over the spectrum zone bigger than 10 μm. Selective surface absorbs approximately 85-95 % of solar radiation (short wave), which turns into heat and is transmitted to the copper plate. However, both copper and copper oxide emit into space only about 10 % of radiation that could be emitted by an

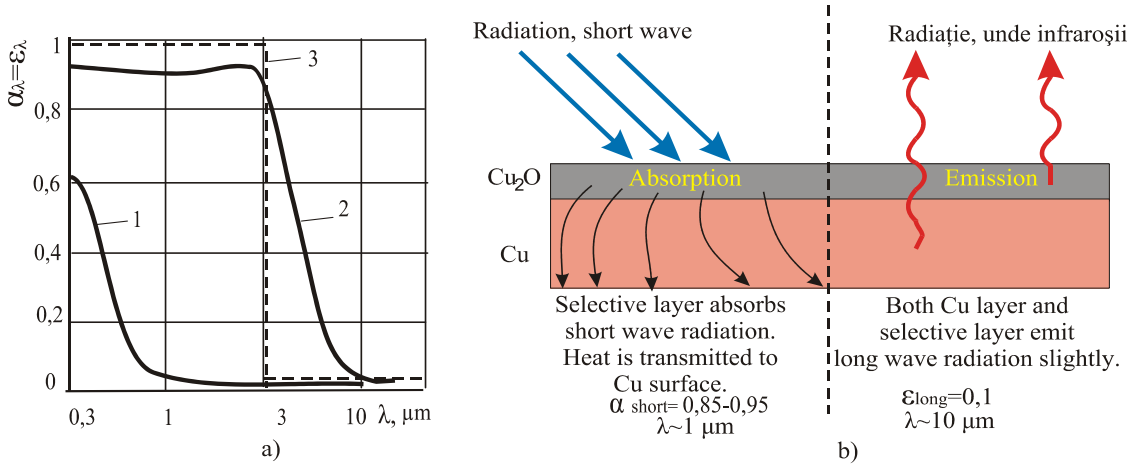


**Fig. 2.10**. Spectral characteristics of different materials (a) and explanation of the selective surface effect (b).

absolutely black body at the same temperature. In other words, selective surface creates the same greenhouse effect as a glass layer covering the solar collector surface. This explains the solar collector efficiency increase with selective surface (Fig. 2.8).

**Transparent surface materials.** Ideal transparent material transmittance is $\tau$=1, its absorbance is $\alpha$=0 and reflectance $\rho$=0. Characteristics of real materials which can be used to manufacture transparent surfaces are shown in Table 2.3. The best quality material for transparent surface is low iron oxide glass or ordinary glass. Glass transmittance drops abruptly for infrared radiation ($\lambda$> 3,0 μm), and, therefore is opaque for radiation emitted by the absorbing surface, thus the greenhouse effect taking place.

Plastics can also be used. They are lighter and cheaper than glass, but age quickly under the action of ultraviolet rays and hence must be replaced periodically (after every 6-12 months). Another plastics disadvantage is low radiative properties. Thus, the polyethylene has an infrared radiation transparency coefficient of 0,8 and therefore will not provide adequate greenhouse effect. The characteristics shown in Table 2.3 are presented for sunbeam incidence angles θ <40° - typical angles for most collectors. Reflectance rises sharply and transmittance reduces for incidence angles bigger than 60°.

**Table 2.3.** Characteristics of transparent materials

| Type of material | Transmittance, $\tau$ | Absorbance, $\alpha$ | Reflectance, $\rho$ |
|---|---|---|---|
| Window glass, 6 mm | 0,80 | 0,12 | 0,08 |
| Float glass (4 mm) | 0,87 | 0,07 | 0,06 |
| Glass with reduced content of iron oxide | 0,91 | 0,01 | 0,08 |
| Polycarbonate | 0,70 | - | - |
| Polyethylene film | 0,82 | - | - |
| Plexiglas (acrylic glass) (3 mm) | 0,80 | - | - |
| Tedlar | 0,88 | - | - |

## Schematic design of solar water heating systems

The most widespread solar water heating systems (SWHS) are shown in fig. 2.11. The basic components of SWHS are: flat solar collector, storage tank (water reservoir), heat exchanger, circulating pump, auxiliary energy source. The difference of the presented diagrams consists in the interconnection and structural arrangement.

**SWHS with natural circulation.** Fig. 2.11 a, shows a SWHS with natural circulation (thermosyphon). To ensure a steady water circulation the storage tank should be mounted higher than the collector. In both components, in the collector and in the water reservoir a difference of temperatures in their upper and lower parts is settled, that leads to a difference of density between the water layers (hot water is easier than cold water) and finally to a pressure difference that ensures water circulation. Pressure difference depends on the temperature difference and thus the water flow in the system depends on the useful power captured by the collector that causes this temperature difference. In these circumstances, SWHS with natural circulation are self-adjustable – the increase in the captured output leads to the increase of the water flow that circulates in the system.

Theoretical and experimental studies carried out in the '70s of the last century have demonstrated [5] that for a wide range of SWHS with natural circulation the temperature difference of water input and output from the collector is about $10^0$C and remains constant during the day. Specific water discharge is 50–60 l/m$^2$h. For example, in a SWHS with the collector's surface 4 m$^2$ water discharge is about 200 l per hour. If storage tank volume is 200-300 l then during a day this volume of water will circulate in the system several times. It is obvious that at the end of the day, the temperature difference between the upper and lower layers water in the tank will be minimum and water circulation will stop. SWHS with natural circulation is widely used in Turkey, Israel, Australia, California and Florida in the USA where there is no danger of frost. The construction of this system is simpler, does not demand additional cost and is designed to heat water at the temperature of $65^0$C. In Moldova, SWHS with natural circulation can be operated from Mart to October. To avoid deterioration of collector it is recommended to empty it from water in the cold period of the year. The auxiliary electrical energy source or the source based on natural gas use allows coverage of hot water over consumption. It can be paralleled with the solar collector (as shown in fig. 2.11, a or in series). In the last case, SWHS operates as pre-heater. It should be mentioned that SWHS with natural circulation will operate with higher efficiency if main hot water consumption will occur in the morning hours. Or, the water reservoir must be filled with cold water before maximum solar radiation occurs.

**SWHS with artificial circulation.** SWHS with pump circulation is shown in fig. 2.11, b. The circulating pump will depend on the temperature difference T2 in the upper part of the collector and temperature T1 in the lower part of the reservoir. Temperature is controlled by a differential relay and the pump will operate only when the temperature difference will overrun the predetermined value. To exclude the reverse circulation of water at night a unidirectional valve is envisaged.

**SWHS with two circulation contours.** In the regions with danger of frost the design of SWHS will be modified and will have two circulation contours. The first contour (fig. 2.11, c) comprises a collector, a circulating pump and a heat exchanger, and it is filled with antifreeze solution. The second contour is the hot water circuit itself. Heat transfer between the first and the second contours is done via a liquid-liquid heat exchanger. This diagram is widely spread in the countries of Central and Northern Europe and in the North America. A standard SWHS comprises 2–3 collectors (their size is 1x2 m), water reservoir volume is 200–400 l, specific water discharge is 50–60 l/m2 h. Solar collector is made of single-layer glass, the absorbing surface is selective, and in some cases is a black surface.

## Practical aspects of solar water heating systems

**Transparent surface (TS) and absorbing plate (AS).** The importance of optical characteristics of materials for manufacturing transparent surfaces and absorbing plates was underlined in paragraph 3.2.4. Properties ($\tau\alpha$) and $\varepsilon$ have a direct impact on thermal

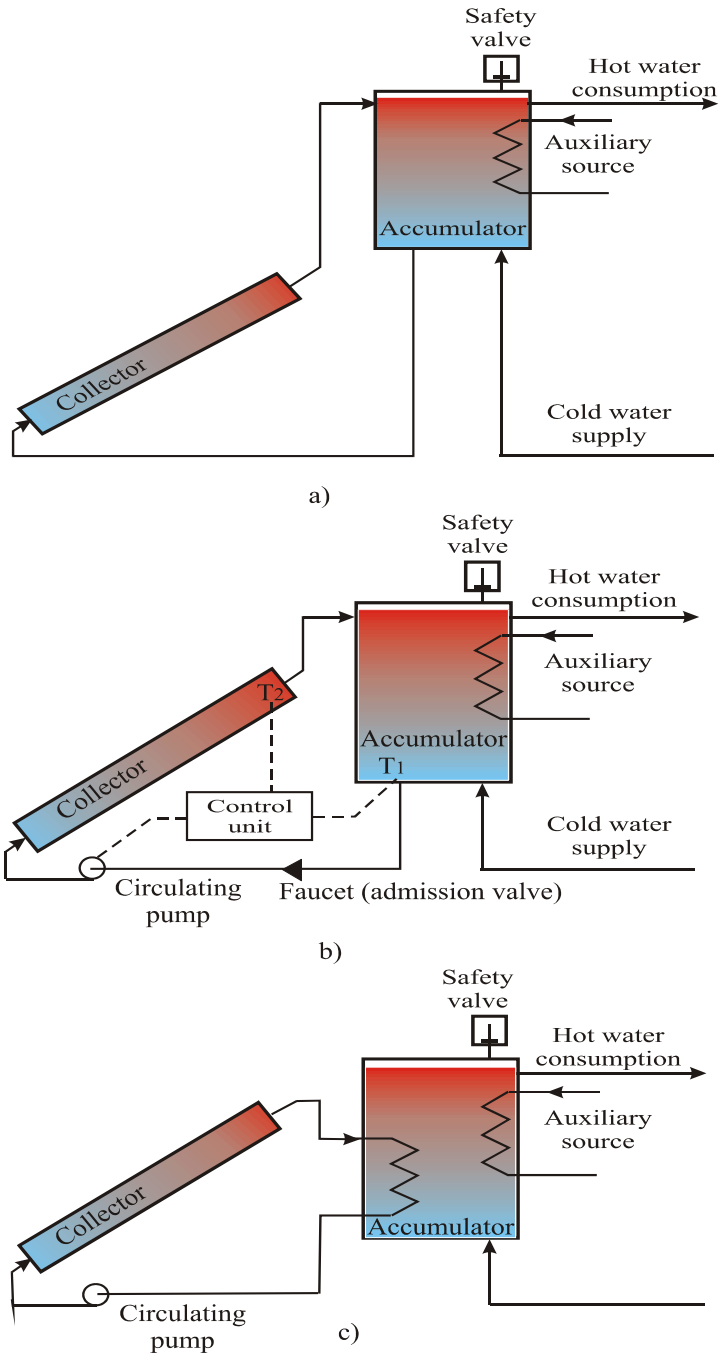


**Fig. 2.11.** Schematic diagram of solar systems for water heating: a – with natural circulation; b – with artificial circulation; c – with two circulation contours

performances of the solar collector. The selected materials should have steady properties in time as their degradation can affect long-term properties of the collector. The surface of the absorbing plate should resist at maximum possible temperatures in the period of exploitation. This can be determined easily from the equation (3.4) under the condition that useful power $Q_u=\eta G$ is equal to zero (there is no water circulation). The fluid temperature $T_m$ will equal the plate temperature. Obviously, the selective material or the applied paint should resist to these temperatures. The combination of glass with the casing should be done without edges or fins that are pointed out above the transparent surface. This would facilitate water flow and snow sliding from the surface of the collector.

**Heat insulation.** Transparent surface (glass) and the air case between AS and TS have the role of heat insulation in the frontal part of the collector. The air case should be within 25

and 40 mm. The thickness 28 mm is considered optimum. The other sides of the collector (the underside and the lateral sides) should be isolated with a 5–10 cm layer of glass wool or other insulating material with similar heat insulation parameters. Glass wool has the following advantages:

- is relatively cheap;
- has excellent insulating properties ($\lambda$ = 0,05–0,06 W/m·K);
- is temperature resistant, over $100^0$C;
- has very small specific mass ($\rho$ = 150–200 kg/m$^3$).

A disadvantage of glass wool is loss of insulating features if it becomes moist. It is recommended to use panels of glass wool and thus settling will be avoided at inclined placement of the solar collector.

A reasonable solution related to cost-quality can be heat insulation combined with a 4 cm glass wool and with another 3 cm panel made of expanded polystyrene. Glass wool is more resistant to higher temperatures, and is placed immediately after the absorbing plate, but polystyrene is placed after the glass wool panel. In its turn, polystyrene is more water resistant. To improve heat insulation of the collector, it is recommended to introduce a thin aluminum sheet between the insulation and the absorbing plate. The sheet will have the role of a screen to infrared radiation that will be reflected to the absorbing plate. An air case between the absorbing plate and the sheet will have the role of additional heat insulator.

**Collector sealing**. To prevent water and dust intrusion into collector, it is necessary to pack it. In conditions of cloudy sky water vapors condense on the internal surface of glass that will lead to decreasing its transparency and efficiency. At next starting of the collector, condensation will disappear only when the glass will become sufficiently warm for its damping. Thus, the collector, which internal air is damp, will start operation later and stop it earlier. If the collector is not sealed the dust will intrude into it and will deposit on the interior side of glass and on the transparent plate. If economically it is difficult to perform perfect sealing then it is recommended to have internal ventilation of the collector. Aiming at this, several holes (2-3 mm diameter) are made between TS and AS that are sheltered from rain.

**Housing.** It supports the unit and ensures collector's sealing. The mostly recommended material is the anodized aluminum angle and zinc steel sheets. The structure of housing does not need high mechanical strength. Usually the collectors are placed on house roofs (fig. 2.12) or are retained by a support made of steel angle profile. This support will take over wind stresses too. The housing is simple in construction and presents a box with flat or undulated ground (for a higher rigidity) and four sides. The height of sides should correspond to the mounting requirements for heat insulation, transparent and absorbing surfaces and an air case, a total height of 10–15 cm. It is important that the housing and collector's weight is small in order to ease its mounting.

**Collectors' mounting** will be in series or parallel (fig. 2.13). At series connection water flows consecutively through collectors and heats more and more. The collectors will operate under various temperatures, with a decreasing efficiency from input to output. Hydraulic resistance is increasing. Due to this, it is recommended for pump circulation systems. When mounted in parallel, each solar collector will ensure only a part of the discharge and will have about the same temperature. Hydraulic resistance decreases and the system can operate under natural circulation. Also hybrid systems with series/parallel or parallel/series connection might be applied.

## 2.2.7. Dimensioning of a solar water heating system

Previously it was stated that SWHS efficiency decreases together with the increase of temperature between the absorbing plate and the environment. It is important to estimate

**Fig. 2.12.** An example of solar water heating system: solar collectors are integrated in the roof of the house directed to the south.

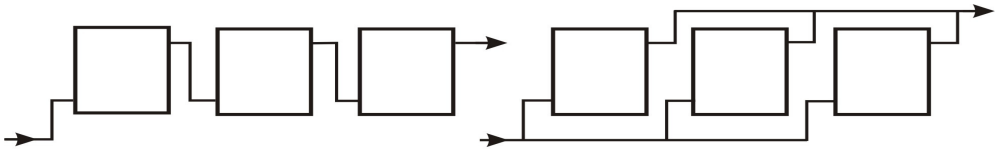

a) b)

**Fig. 2.13.** Connection of solar collectors, in series (a) and parallel (b).

correctly the dimension of solar collector's surface and the volume of water reservoir depending on the:

- available overall radiation on the collector's surface;
- daily hot water consumption and temperature;
- distribution of water consumption over the day.

Further on, a simple method for dimensioning is described. This method allows preliminary SWHS estimation, in particular, at the first stage of designing solar energy systems, inclusive feasibility studies. SWHS diagram is shown in fig. 2.11, a. It has a single contour with natural circulation. The dimensioning estimates refer to the following sizes:

- optimum slope angle of solar collectors for the given period: March to October, central regions of Moldova;
- average global radiation for the given period incident on collector's surface and monthly average global radiation;
- daily consumption of hot water and its distribution for 24 hours;
- solar collector surface;
- volume of hot water storage reservoir;
- minimum water temperature per month with smaller solar radiation.

The optimum slope angle of solar collectors is chosen so as in March and October more solar energy is radiated to the collector's surface, and care is taken that in summer this quantity of energy does not decrease under the required level.

**Overall average radiation incident on the collector's plane.** Average daily values of direct and diffuse solar radiation on a horizontal surface for the period from March to October are taken from local characteristics. Diffuse radiation is determined as the difference between

the overall and direct radiation. Global radiation on the collector's surface is determined from the expression (2.25), neglecting the reflected component:

$$G_\beta = R_b \cdot B + \frac{1}{2}(1 + Cos\beta)D\,. \qquad (3.15)$$

The obtained results are included in table 2.4.

**Table 2.4.** Overall radiation at the collector surface for the studied period

| Month | | III | IV | V | VI | VII | VIII | IX | X |
|---|---|---|---|---|---|---|---|---|---|
| $R_b$ | - | 1,57 | 1,15 | 0,93 | 0,85 | 0,88 | 1,06 | 1,38 | 1,94 |
| $B$ | $MJ/m^2 \cdot zi$ | 4,22 | 7,34 | 10,26 | 13,03 | 12,55 | 11,24 | 8,51 | 4,78 |
| $D$ | $MJ/m^2 \cdot zi$ | 5,57 | 7,98 | 9,32 | 10,05 | 9,55 | 8,06 | 6,14 | 4,3 |
| $B_\beta=R_bB$ | $MJ/m^2 \cdot zi$ | 6,63 | 8,44 | 9,54 | 11,07 | 11,04 | 11,91 | 11,74 | 9,27 |
| $D_\beta=1/2(1+Cos\beta)$ | $MJ/m^2 \cdot zi$ | 4,86 | 6,96 | 8,13 | 8,76 | 8,33 | 7,03 | 5,35 | 3,75 |
| $G_\beta=B_\beta+D_\beta$ | $MJ/m^2 \cdot zi$ | 11,49 | 15,4 | 17,67 | 19,83 | 19,37 | 18,94 | 17,09 | 13,02 |
| | $kWh/m^2 \cdot zi$ | 3,20 | 4,31 | 4,95 | 5,55 | 5,42 | 5,30 | 4,79 | 3,64 |

**Daily consumption of hot water and its distribution for 24 hours.** Daily demand for hot water and its distribution for 24 hours depend, to a great extent, on the consumer's specific characteristics. It is different for houses and industrial buildings. Assuming as consumer a family of four persons, the specific consumption $q$ is 50 l/day per capita at the temperature $55^0$C. The distribution of water consumption for 24 hours is shown in table 2.5 [7].

**Table 2.5.** Home hot water 24 hour consumption

| Hour | Consumption, % | Hour | Consumption, % | Hour | Consumption, % |
|---|---|---|---|---|---|
| 0-1 | 0,0 | 8-9 | 4,6 | 16-17 | 4,2 |
| 1-2 | 0,0 | 9-10 | 4,4 | 17-18 | 4,5 |
| 2-3 | 0,0 | 10-11 | 3,9 | 18-19 | 5,7 |
| 3-4 | 0,0 | 11-12 | 4,0 | 19-20 | 7,8 |
| 4-5 | 0,0 | 12-13 | 4,6 | 20-21 | 9,1 |
| 5-6 | 3,0 | 13-14 | 4,6 | 21-22 | 9,1 |
| 6-7 | 5,2 | 14-15 | 4,6 | 22-23 | 6,5 |
| 7-8 | 5,4 | 15-16 | 4,0 | 23-24 | 4,7 |

The data in table 2.5 and the daily consumption of 4·50 = 200 l/day defines the distribution of hot water consumption *C(t)* during the day by summing the values for each hour. The results are introduced in table 2.6, graphic presentation is given in fig. 2.14. The same graph shows cumulative production of hot water from period $7^{30}$ - $18^{00}$.

**Table 2.6.** Daily distribution of hot water consumption, *C(t)*.

| Hour | | 0 | 4 | 6 | 8 | 10 | 12 | 14 | 16 | 18 | 20 | 22 | 24 |
|---|---|---|---|---|---|---|---|---|---|---|---|---|---|
| C(t) | % | 0,0 | 0,0 | 3,0 | 13,6 | 22,6 | 30,5 | 39,7 | 48,3 | 57,0 | 70,5 | 88,7 | 99,9 |
| | l | 0,0 | 0,0 | 6,0 | 27,2 | 45,2 | 61,0 | 79,4 | 96,6 | 114,0 | 141,0 | 177,4 | 200,0 |

**Solar collector surface.** The energy demanded to heat the daily water volume *Cz* = 200 l from $15^0$C to $55^0$C is estimated:

$$E_{nec.} = C_z \cdot c_{water}(t_{hot} - t_{cold}) = 200 \cdot 4{,}173 \cdot 10^3 \cdot 40 = 33{,}39\ MJ/day,$$

where $c_{water}$ = 4,173·103 J/$^0$C·kg is the water specific heat.

Capture surface of the solar collector:

$$S_{col} = \frac{E_{nec}}{\eta_{col} \cdot G_{\beta med}} = \frac{33,39}{0,45 \cdot 16,6} = 4,5m^2,$$

where $\eta_{col}$ is collector average efficiency for the period of operation; $G_{\beta med}$ – daily global solar radiation determined as the average for the period from March to October (see data in table 2.4).

**Volume of hot water storage tanks.** Fig. 2.14 shows that the storage tank should supply the hot water production deficit from 5 to 8 o'clock in the morning, and from 18 to 24 o'clock in the evening. Thus, the storage tank volume is:

$$V_a = V_1 + V_2 = 30 + 90 = 120\ l.$$

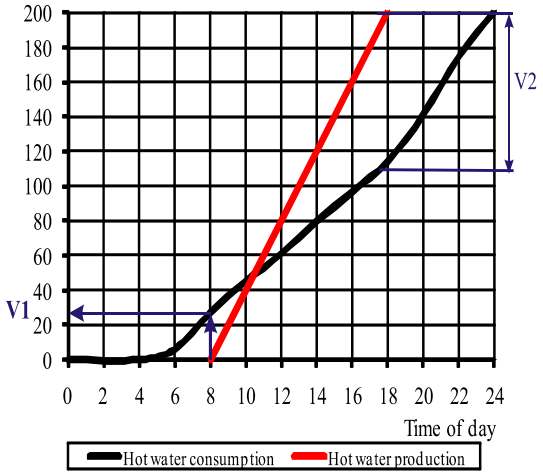


**Fig. 3.14.** Explanation of hot-water tank volume determination

The temperature of hot water in March when solar radiation is the smallest:

$$t_{hot} = t_{cold} + \frac{C_{\beta}^{III} \cdot S_{col} \cdot \eta_{col}}{C_z \cdot c_{water}} = 10 + \frac{11,69 \cdot 10^6 \cdot 4,5 \cdot 0,45}{200 \cdot 4,173 \cdot 10^3} = 38,4^o C.$$

So, one can see that in March a comfortable temperature of hot water for residential purposes is also supplied.

**Quantity of thermal energy produced from March to October** is determined from the expression:

$$E_{III-X} = N_z \cdot G_{\beta med} \cdot S_{col} \cdot \eta_{col} = 245 \cdot 16,6 \cdot 4,4 \cdot 0,45 = 8053\ Mj$$

or about 2 Gcal.

## 2.3. Solar systems with solar concentrating collectors

### 2.3.1. Brief history

The power density of solar radiation on the earth's surface rarely exceeds 1000 W/m$^2$. Using plane collectors analyzed above, it becomes impossible to obtain temperatures greatly exceeding 100ºC. Temperatures of hundreds or even thousands degrees can be obtained only through the concentration of solar radiation direct component.

Legend says that in 212 BC Archimedes used for the first time the effect of sunlight concentration. With polished-to-shine soldier shields (thus becoming genuine bronze mirrors) sunlight was reflected and concentrated in such a manner that allowed burning the Roman ships besieging the Syracuse fortress. In order to verify the legend, in 1973 the Greek Naval Authority showed how 60 people, each with a mirror sizing 1x1.5 m (1.5 m$^2$), burned a wooden ship situated at 50 m distance. If during the experiment the radiation density was about 800 W/m$^2$, than in the centre it was about 0,8x1,5x60 = 72 kW/m$^2$, thus exceeding 1,5 times the power density on the surface of an electric heating plate.

This way of capturing solar energy always is in the attention of researchers. L. Stoddard and others have conducted extensive studies on the economic, environmental and

energy benefits of sunlight concentrating systems [8,9]. The largest group, which focuses on research and use of concentrated sunlight solar systems, is U.S. Solar Energy Generating Systems (SEGS), which developed and built in the Mohave Desert of southern California parabolic systems with a total capacity of 354 MW. These systems functioned very well during 15-20 years. Today SEGS has a number of commercial projects under development or under construction, including a 64 MW parabolic system in Nevada and several 50 MW systems in Spain. Integrated systems are at various planning stages in Southern California, India, Egypt, Morocco, Mexico and Algeria. A parabolic system has recently been built for Arizona Public Service [10].

In 2005, Southern California Edison company announced the completion of contract negotiations with Stirling Engine Systems (SES) company for the purchase of 1182...2010 GWh per year for a period of 20 years. As a result of large-scale development of these parabolic systems with Stirling engines significant reduction of capital and operating, as well as maintenance costs are expected [10]. Detailed information on sunlight concentration solar systems can be found in [10, 11].

In general, three basic types of solar power plants with sunlight concentration are known: cylindrical-parabolic systems (with gutters); with parabolic mirrors and Stirling engine; solar towers with heliostat concentrator.

## 2.3.2. Thermal conversion of solar energy at high temperatures: theoretical issues

Operation of solar concentrators is based on two phenomena studied by physics: reflection and refraction of light. If a surface is not rough or the linear sizes of a surface are much smaller than the wavelength of an incident light beam, this surface reflects. Surface reflection capacity is characterized by the reflectance factor. Reflectance values for common materials are:

- galvanised silver – 0,96;
- pure aluminium – 0,91;
- silver deposited on the inner surface of the glass (mirror) – 0,88;
- silver deposited on the outer surface of the glass – 0,93;
- posterior surface aluminized acrylic film – 0,85.

**Parabolic mirror.** This is a concave mirror (Fig. 2.15), which surface is described by the parabola $y^2 = 2cx$ around the optical axis $x$. Figure obtained is called paraboloid. A cylindrical-parabolic mirror is obtained if parabola is moved in the direction of $z$ axis. Rays of light parallel to the optical axis $x$, incident on reflective surface, concentrate in point $F$, called focus point.

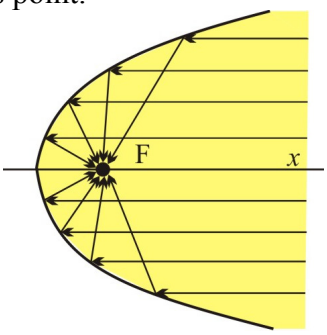


**Fig. 2.15.** Parabolic mirror

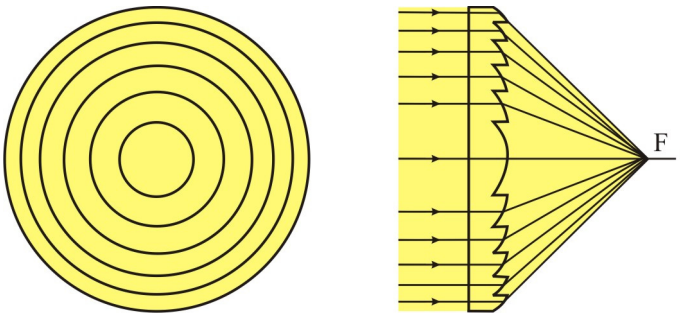


**Fig. 2.16.** Fresnel lens

**Fresnel lens.** This is a unit composed of several concentric lenses (Fig. 2.16), which functions as an integral lens. Material and mass costs of a Fresnel lens are much smaller than those of a conventional one. Parallel light flux concentrates in focus point *F*.

The solar energy concentrators, used in thermal conversion, are composed of three main components: the reflector that receives sunlight and directs in to the focus point; the receiver, located in the focus point and that turns sunlight into heat; sun position tracking system. Fresnel type concentrators are used in the photovoltaic technology of solar energy conversion only.

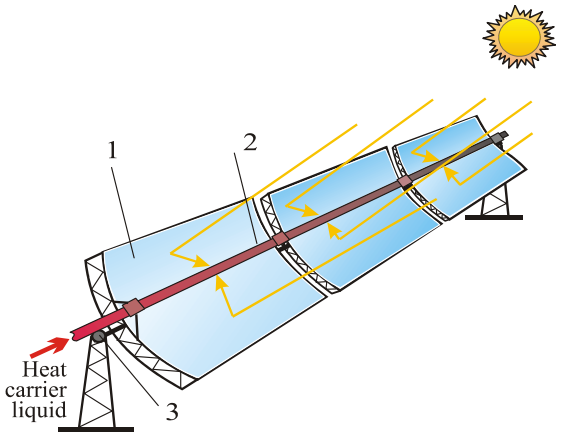


**Fig. 2.17.** Operating principle of cylindric-parabolic concentrator

The basic parameters that characterize a solar concentrator are concentration coefficients. Geometric concentration coefficient is the ratio between surface area open to sunlight, or aperture $A_a$, and receiver's surface area, $A_r$:

$$C_g = \frac{A_a}{A_r}. \tag{3.16}$$

Optical concentration coefficient is the ratio between the power density of direct radiation on the receiver's surface, $B_r$ and power density of direct radiation on the aperture $B_a$:

$$C_r = \frac{B_r}{B_a}. \tag{3.17}$$

For an ideal concentrator $C_g = C_r$, in fact $C_r < G_g$. Taking into consideration the distance between the earth and the sun disk diameter, the geometric concentration factor cannot be bigger than:

$$G_g < \left(\frac{2L}{D_s}\right)^2 = 45000\,. \tag{3.18}$$

Fig. 2.17 shows a design diagram of the concentrator with three cylindrical-parabolic reflective mirrors 1 (in the form of a gutter). Solar radiation receiver 2 represents a pipe through which the thermal agent fluid, usually water, circulates. The receiver 2 is mounted in the focus point of the parabolic cylinder, representing a line crossing the optical focus point *F* of the parabola from Fig. 2.15. An important feature of the cylindrical-parabolic concentrator is the tracking of only one coordinate from sun trajectory - elevation angle $\alpha_s$. In the construction from Fig. 2.16, tracking is done by rotating mirror 1 around the axis 3. Receiver temperature reaches 400 - 500ºC.

The second concentrator type (Fig. 2.18) has a parabolic mirror 1 (in the form of a plate), serving as a reflector. The receiver 2 is mounted in the paraboloid focus point. The orienting mechanism (not shown) must ensure tracking of two angles - elevation $\alpha_s$ and azimuth $\gamma$. Receiver temperature can reach over a thousand degrees. The heat collected is usually used directly by thermal engine mounted on the receiver, which moves with the plate unit.

Concentrators of this type are used for melting and obtaining of most pure metals in ground conditions or for electricity generation. Stirling or Brayton heat engines are usually used as heat engines. Such modular systems with total capacity of up to 5 MWe have been

manufactured. Maximal power registered for a module is about 50 kWe, achieving an efficiency of up to 30 %.

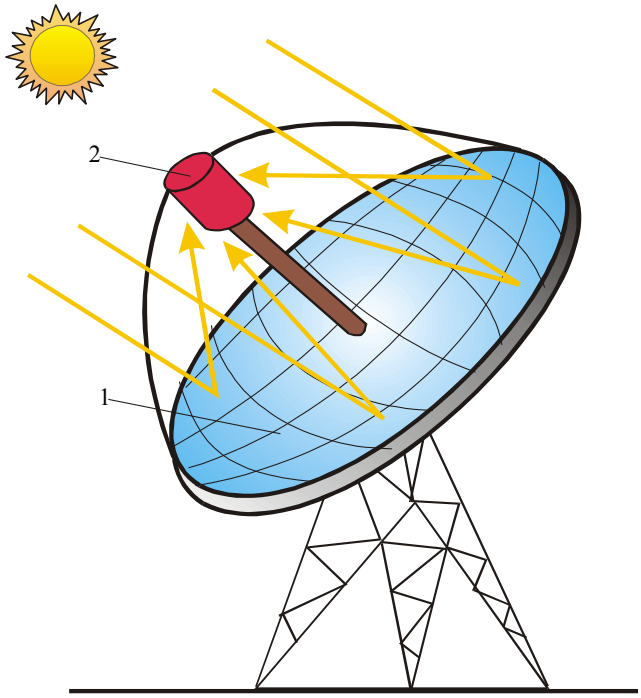


**Fig. 2.18.** Operating principle of solar concentrator with parabolic mirror

The main advantages are:

- rotation mechanism around two axes allows to collect the maximum sunlight quantity;
- easily transported and assembled modular construction;
- highest efficiency compared to any other generating solar technologies;
- requires limited areas;
- long operation period.

Heliostat concentrator is the equivalent of a very large parabolic concentrator (Fig. 2.19). Heliostats 1, small flat-shaped reflectors, are located around the entire circumference of the central tower forming the so-called heliostat field. The reflector 2 is mounted on the tower in the paraboloid focus point. Each heliostat is remote-controlled and follows the two coordinates of the sun position. The first heliostat concentrator was built in 1949 under the supervision of the French professor, Felix Trombe, in Mont-Luis area in the Pyrenees [12].

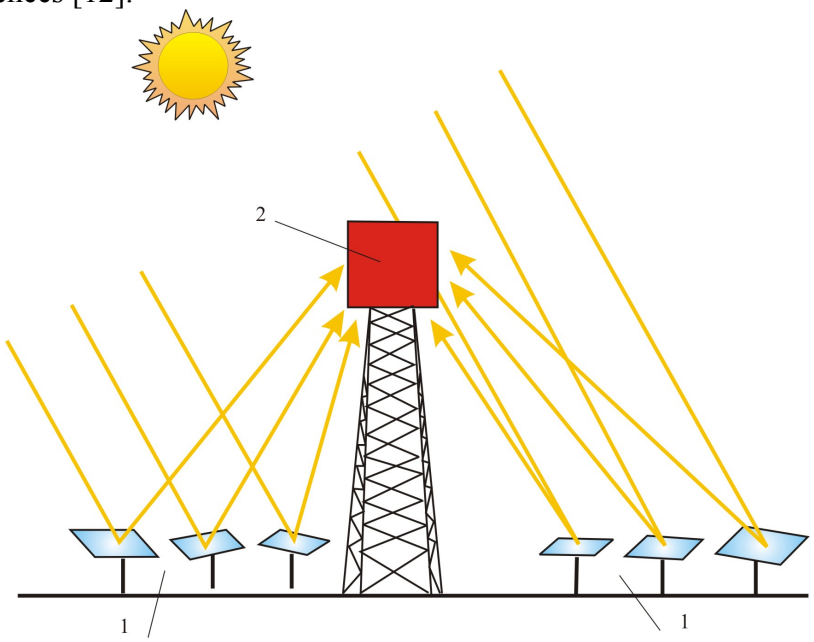


**Fig. 2.19.** Operating principle of the concentrator with heliostate.

The heliostat field was situated on 130 $m^2$, receiver power reached 50 kW, and the temperature reached 3000-4000 ºC. The facility aimed the study and creation of new materials, in particular of composite materials.

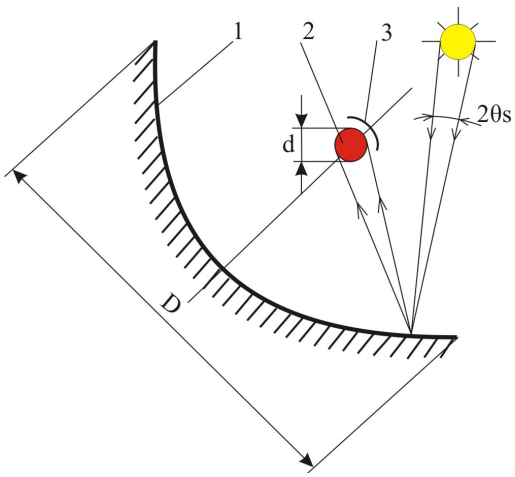


**Fig. 2.20.** Simplified diagram of the parabolic concentrator

To estimate the temperature of the receiver we use Fig. 2.20, which depicts a simplified diagram of parabolic mirror concentrator: 1 is a cylindrical-parabolic or paraboloid mirror, 2 - receiver placed in the paraboloid focus point. 3 – receiver screen. Cylinder-parabolic mirror has length $l$ and opening $D$, and in the case of paraboloid mirror - aperture diameter is equal to $D$. The receiver of cylinder-parabolic concentrator represents a pipe with diameter $d$ and length $l$, or has a spherical shape with diameter $d$ for paraboloid concentrator. Solar disk angular size is equal to $2\theta_s$, where $\theta_s = R_s / L$.

**Temperature of the cylindrical-parabolic concentrator receiver.** The power of solar radiation absorbed by the receiver:

$$P_{abs} = \rho_c \alpha l D B, \tag{3.19}$$

where $\rho_c$ is the reflectance of mirror surface, $\alpha$ - absorption of receiver; $B$ - direct solar radiation. The receiver, having the temperature $T_R$, emits radiant power in space, which, according to Stefan-Boltzmann law, is determined by the expression 2.6:

$$P_{rad} = \varepsilon \sigma T_R^4 \pi d l (1 - \zeta / \pi), \tag{3.20}$$

where $\varepsilon$ is the receiver emissivity; $\sigma$ - Stefan-Boltzmann's coefficient, $\xi$ - shielding factor of receiver, usually $\xi = 2/3\pi$, $d$ - diameter of the receiver, determined by the opening $D$: $d = D\theta_s$.

At steady heat condition absorbed power is equal to the radiated power (other power losses of the receiver are neglected), from where the maximum temperature of the receiver is determined:

$$T_R = \sqrt[4]{\frac{\rho_c \alpha B}{\varepsilon \sigma \theta_s}}. \tag{3.21}$$

For $B$ = 600 W/m$^2$, $\alpha/\varepsilon$ = 1, $\rho_c$ = 0.8, $\sigma$ = 5.67 W·m$^2$·K$^{-4}$, $\theta_s$ = 0.00465 Rad, maximum temperature of 1162 or 889 ºC is obtained. In usual systems with cylindrical-parabolic concentrators temperatures up to 700 ºC are obtained. Temperature decrease is due to mirror surface deviation from the ideal parabolic shape and to the fact that liquid thermal agent circulating through the receiver, leads to $P_{rad}$ decrease.

**Temperature of paraboloidal concentrator receiver.** A sphere-shaped receiver with a diameter $d$ is considered, other sizes and assumptions remain the same as in the previous case. From the thermal balance condition we obtain:

$$T_R = \sqrt[4]{\frac{3\rho_c \alpha B}{8\varepsilon \sigma \theta_s^2}}. \tag{3.22}$$

For the same amount of direct solar radiation $T_R$ = 3480 ºK or 3208 ºC are obtained. In real plants temperatures up to 3000ºC can be obtained.

## 2.3.3. Heat engines used at solar thermal plants

**Solar thermal system with steam engine.** Conversion of solar thermal energy into mechanical energy or electricity was the goal of experiments for over a century. At 1872 Paris exhibition professor of mathematics Augustin Mouchot and engineer Abel Pifre presented the first system converting solar energy into mechanical energy - a printing press driven by a steam engine powered by a solar parabolic concentrator (Fig. 2.21). Later, in 1913, American entrepreneur Frank Shuman applies the same principle in Egypt, manufacturing the first solar unit for irrigation [12, 13]. The steam for the thermal engine was generated by 5 cylinder-parabolic collectors with an 80 m length and 4 m aperture each. The receiver – a cast iron pipe situated in the focus point, provides transportation of the steam to the engine. The unit develops a mechanical power of about 45 kW, which was used to pump water from river Nile

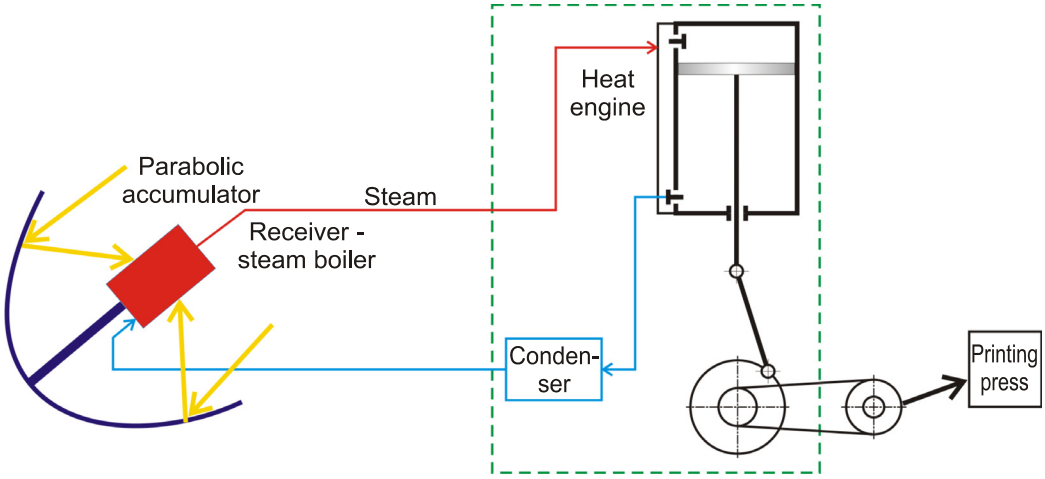


**Fig. 2.21.** Schema of solar thermal engine elaborated by Augustin Mouchot and Abel Pifre în anul 1872

for irrigation. Due to the high price of coal in that area at that time, system recovery period did not exceed four years.

It is necessary to note one very important disadvantage of solar steam engines - low efficiency. It follows from the low power density of solar radiation and the fundamental principles of thermodynamics. A more understandable interpretation of the second law of thermodynamics states: thermal or heat energy cannot be fully converted into other forms of energy, such as mechanical or electrical. The efficiency of a piston or turbine heat engine depends on the warm source temperature, i.e. input temperature $T_{in}$ and cold source temperature (condenser) $T_{out}$, between which heat exchange occurs. Maximum efficiency or maximum Carnot efficiency can not exceed the value obtained from the expression:

$$\eta_C = 1 - \frac{T_{out}}{T_{in}}. \qquad (3.23)$$

For example, a turbine powered by a steam parabolic concentrator at a 350 ºC temperature and a 30 ºC condenser temperature shall have a theoretical efficiency equal to 1-(30+273)/(350+273)=0,51 or 51 %. Real efficiency, due to energy losses shall not exceed 25 %.

To obtain water vapors a temperature of at least 100 ºC is required. If temperature obtained from the solar collector is lower, than a heat engine employing Rankine cycle can be used. Here, as fluid thermal agent, organic substances are used that boil at below 100 ºC and used in refrigerators and heat pumps. Such a heat engine shall have an even lower efficiency.

For example, a heat engine efficiency operating on 85ºC vapors, obtained from a plate solar collector, and at 30 ºC condensing temperature shall not exceed 15 %.

**Solar thermal system with steam turbine.** World War I caused the widespread use of internal combustion engines operating on petrol or diesel. Cheap oil era began and solar thermal systems have been forgotten for a period for over 50 years. They returned after the start of the 1973 oil crisis. A group of U.S. engineers led by G. Alexander performed in 1979 a new solar irrigation project in the Gila Bend area [5]. Fig. 2.22 shows the operation scheme of this system. Primary energy is obtained from a 537 $m^2$ cylindrical-parabolic solar collector, which heats water to a temperature of 150 ºC at about 7 bar pressure. The hot water circulates through the heat exchanger, working as a boiler too, pre-heater and receiver. In the secondary circuit (not shown in the diagram) of the heat exchanger, the working fluid Refrigerant 113 with a low boiling temperature is used. The vapors with 138 ºC temperature and about 9 bar pressure are used to power a turbine which drives the pump. Part of vapors is used to preheat the water in the primary circuit. After the turbine vapors are used in the regenerator to heat the water from the preheater circuit. The regenerator vapors condense in the condenser, where part of the water pumped is used for cooling and at a temperature of about 32 ºC is returned to the tank. In the first year of operation, the system worked for 323 hours at a capacity between 240 and 570 l/s or 364 and 2052 $m^3$/h. In the second year it worked for 188 hours, delivering 1.24 x$10^5$ $m^3$ [5] or at a capacity of 660 $m^3$/h.

## 2.3.4. Solar thermal power plants (STPP) with cylindrical-parabolic concentrators

The conversion of solar thermal energy into electricity is similar to the traditional conversion, based on fossil fuels where energy stored in the fuel is released through combustion, and is converted into potential energy of compressed and heated to 500-600 ºC steam. In the turbine, the steam expands, the potential energy turns into kinetic energy which, in its turn, transforms into electricity. In solar systems, fossil fuel is replaced by solar radiation, boiler combustion chamber - with a concentration solar collector: cylindrical-parabolic, with parabolic mirror or with heliostat and central tower. Solar thermal collectors with focused sunlight are mainly used to generate electricity. There are various systems that differ in the way how they collect and concentrate solar rays, but the final step of generating electricity is identical to that of conventional power plants. Finally, the heat engine is used to convert heat into electricity. The solar system is designed to focus solar rays and transform them into heat, which is used in the heat engine. In a simple way, solar thermal plant is a conventional power unit that uses solar energy as primary source of heat. In the last two decades of the previous century in the U.S. several STPP pilot projects have been successfully completed, which proved their technical and technological viability and paved the way towards new projects with hundreds of MW capacity. Next, a brief description of certain commercial projects with cylindrical-parabolic concentrators is given [5, 13, 14].

The largest solar thermal plant in the world has a maximum power of 354 MW and is located in the Kramer Junction area, California, USA [14]. It was built by Luz International Company in 1985-1991 and consists of 9 units with an electric capacity between 14 and 30 MW. Later this type of plant was called LUZ solar system. Fig. 2.23 shows a part of cylindrical-parabolic concentrators' field. By 2001 the facility supplied in the public network of California 9 TWh of electricity. The plant is equipped with an auxiliary circuit, operating on natural gas and allowing expansion of energy production by 25% either on cloudy weather or during peak hours. The plant was designed to provide electricity during peak hours, when the cost of delivery is the highest.

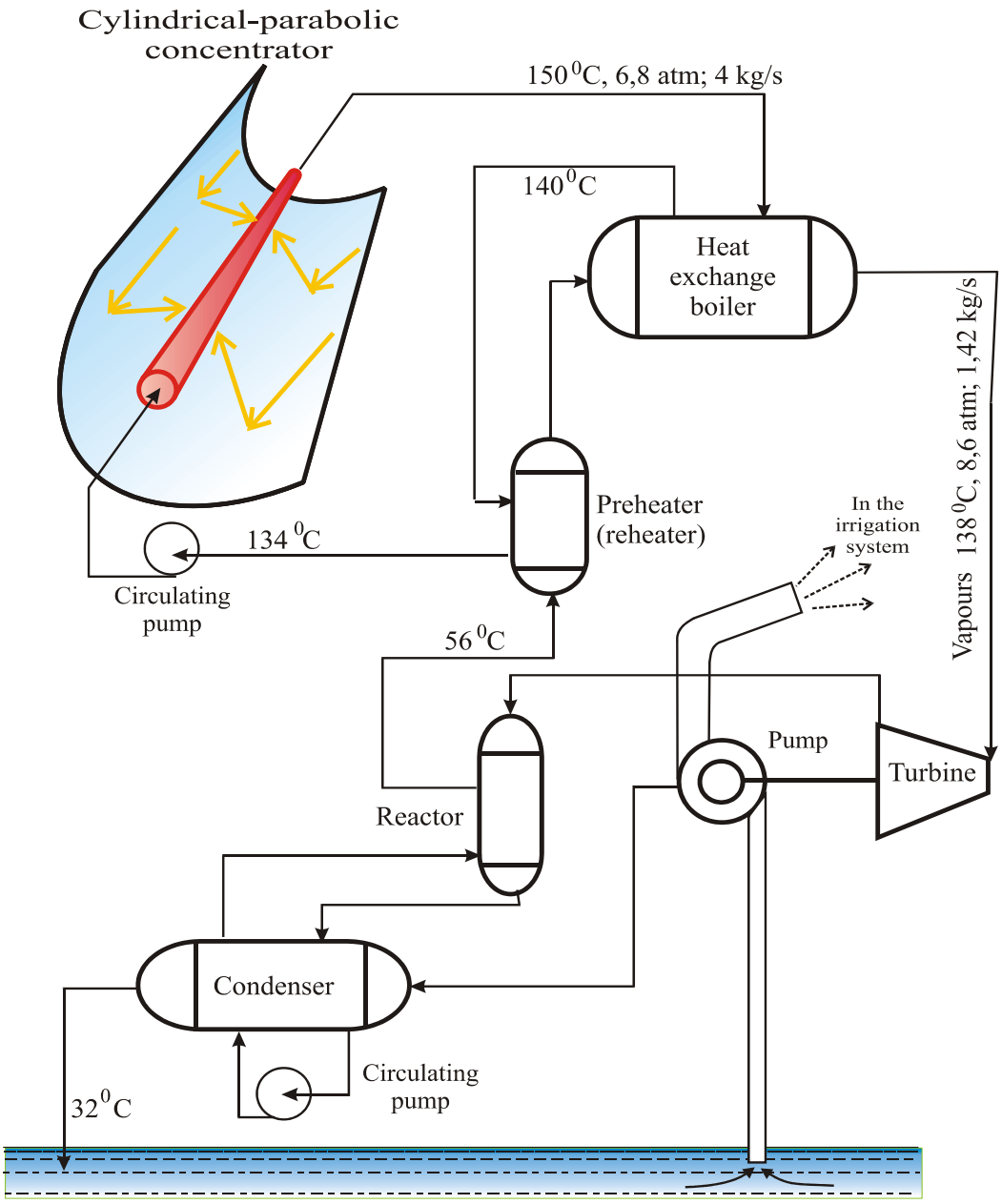


**Fig. 2.22.** Solar pumping system, manufactured by G. Alexander in 1979.

a)

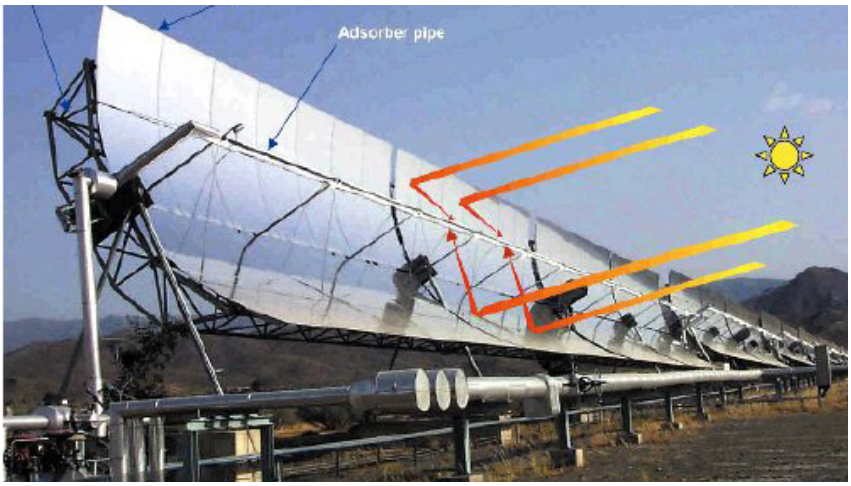


b)

**Fig. 2.23.** Fragment of field with cylindric-parabolic solar collectors of the thermal power plant Kramer Junction (a) and a separate line (b), California [14].

In California this period lasts from June to September, 12:00-18:00 hours. Main plant components are shown in Fig. 2.23. Solar collector field is composed of cylindrical-parabolic (trough) concentrators with a total area of about 1,75 x$10^6$ $m^2$. The active part of the concentrator - the reflector is composed of low-iron glass and coated with silver at the back. Glass is mounted on a metal sectioned frame, which allows the formation of different length collectors. The collectors are mounted in parallel rows in the south-north direction. The sun is tracked using hydraulic drives. The solar radiation receiver has a 70 mm steel tube in diameter covered with a layer of selective material. To reduce energy losses, the receiver is placed in a vacuum glass tube. At a temperature of 350 ºC, the surface receptor has an absorbance equal to 0,96 and an emittance of 0,19 only. Reflectance of clean mirrors is equal to 0,94. In the first contour, which includes solar collectors, a synthetic fluid (usually oil) is used as thermal agent. The fluid leaving the collector has a temperature of 390 ºC, and at the entrance of the collector - about 304 ºC. In the second circuit water turns to steam into the boiler supplied with thermal energy from solar collectors. The generating unit represents a traditional group 'steam turbine-synchronous generator'. Steam turbine has two pressure stages - the first is supplied with superheated steam and the second - from the preheater.

## 2.3.5. Solar thermal power plants with heliostats and central tower

Solar thermal power plants with heliostats and central tower (or, in short, solar towers) use thousands of mirrors called heliostats, which redirect concentrated solar light to the receiver that is installed at the top of the tower. With most receivers, salt solution heated in the receiver is used to generate steam directly into the receiver, steam that is used by a conventional turbine generator to produce electricity. Molten nitrate salt possesses heat transfer properties and has superior energy storage capacity. Commercial power towers can be sized to produce from 50 to 200 MW power. Fig. 2.24 shows the technological scheme of high temperature solar receiver solar tower. In the 90s of the last century several pilot plants with heliostats and central tower were built: in the former USSR – employing 5 MW power; in Italy, Spain and France – employing 1 MW power. The world's largest heliostat plant was built in 1982 in the U.S., Barstow district, California. The plant was called Solar One and has a 10 MW capacity [14, 16, 17]. A general view of the plant is shown in Fig. 2.25. After six years of operation, in 1988 it was decided to rebuild the plant. It was equipped with molten

salt; heliostats control system has also been modernized. Heliostat field includes 1818 reflectors with a total area of 71100 $m^2$. Each heliostat is oriented so as to reflect sunlight on to the receiver installed in the centre of the field at 90 m above the ground. A heliostat includes 12 concave panels with a total area of 39,12 $m^2$. Glass coated with silver was used as reflecting material. The receiver is a 13,7 m height - and 7 m diameter cylinder. The receiver cylinder consists of 24 panels, each having a 0,9 m width and 13,7 m height.

An interesting European project, similar to the above, is the tower which was built in Spain, Solúcar PS10, the first commercial application of the technology [18]. At PS10, 624 heliostats, 120 square meters each, concentrate solar radiation at the top of a 115-meter tower. The concentration rate is about 3000 suns. When completed in 2012, the entire Solúcar facility, called the Sanlúcar La Mayor Solar Platform, will generate more than 300 megawatts of solar power, using tower and cylindrical-parabolic solar collectors along with photovoltaic installations.

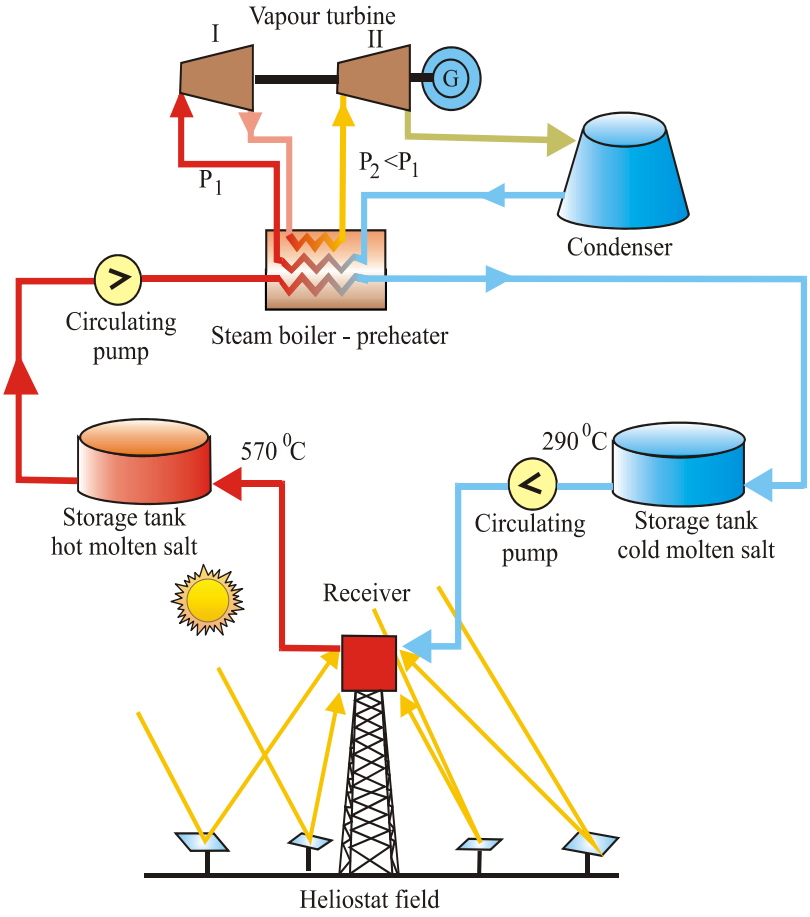


**Fig. 2.24.** Operation principle of solar thermal plant Solar Two

**Fig. 2.25.** Solar thermal plant Solar Two [17].

# References


1. *Experience, prospects and recommendations to overcome market barriers of parabolic trough collector power plant technology Status/Report on Solar Trough Power Plants.* Sponsored by the German Federal Minister for Education, Science, Research and Technology under Contract No. 0329660. Pilkington Solar International GmbH. - 1996
2. Bougard J. *Conversion d'energie. Machines solaires.* Faculte Politechnique de Mons, AGADIR, 1995.
3. Roger A. Hinrichs, Kleinbach M. *Energy: its use and environment.* Third edition. Thomson Learning, 2002, 590 p.
4. Boyle G. *Renewable Energy: power for a sustainable future.* Oxford University Press, 2004, 452 p.
5. John A. Duffie, William A. Beckman. *Solar engineering of thermal proceesses*. – 2nd edition, A Wiley Intersciance Publication, 1991.
6. John W. Twidell and Anthony D. Weir. *Renewable Energy Sources.* – 2nd ed. Taylor & Francis. London. - 2006.
7. Dumitraşcu Gh., Macri V., Stadoleanu O. *Utilizarea energiei solare.* Ed. "Timpul", Iaşi.- 1998.
8. Executive Summary: *Assessment of Parabolic Trough and Power Tower Solar Technology Cost and Performance Forecasts.* Sargent & Lundy LLC Consulting Group Chicago, Illinois NREL Technical Monitor: H. Price. Prepared under Subcontract No. LAA-2-32458-01.
9. *Solar Energy Systems.* Status Report on Solar Trough Power Plants, 1996.
10. Stoddard L., Abiecunas J., O'Connell R. *Economic, Energy, and Environmental Benefits of Concentrating Solar Power in California.* May 2005 – April 2006. Black & Veatch Overland Park, Kansas NREL Technical Monitor: M. Mehos. Prepared under Subcontract No. AEK-5-55036-01
11. www.stirlingenergy.com.
12. Bougard J., Benallou A. *Le solaire thermique au service du developpment durable.* Sous la direction scientifique: IEPF, Quebec, Canada, 1998.
13. www.nrel.gov/docs/fy01osti/28751.pdf
14. www.powerfromthesun.net
15. http://ec.europa.eu/research/energy/pdf/stpp_solair_en.pdf
16. *Concentrating Solar Power: Energy from Mirrors.* DOE/GO-102001-1147, FS 128, March, 2001.
17. *Solar Two Central Receiver.* Consultant report. October, 1999. California Energy Comission.
18. www.technologyreview.com/spain